



HAL
open science

Thermoelectric Properties of the Homologous Compounds $\text{Pb}_5\text{Bi}_6\text{Se}_{14-x}\text{I}_x$ ($x = 0.0, 0.025, \text{ and } 0.05$)

Selma Sassi, Christophe Candolfi, Anne Dauscher, Bertrand Lenoir

► **To cite this version:**

Selma Sassi, Christophe Candolfi, Anne Dauscher, Bertrand Lenoir. Thermoelectric Properties of the Homologous Compounds $\text{Pb}_5\text{Bi}_6\text{Se}_{14-x}\text{I}_x$ ($x = 0.0, 0.025, \text{ and } 0.05$). *Journal of Electronic Materials*, 2018, 47 (6), pp.3198-3202. 10.1007/s11664-018-6061-8 . hal-02391388

HAL Id: hal-02391388

<https://hal.science/hal-02391388v1>

Submitted on 24 Mar 2020

HAL is a multi-disciplinary open access archive for the deposit and dissemination of scientific research documents, whether they are published or not. The documents may come from teaching and research institutions in France or abroad, or from public or private research centers.

L'archive ouverte pluridisciplinaire **HAL**, est destinée au dépôt et à la diffusion de documents scientifiques de niveau recherche, publiés ou non, émanant des établissements d'enseignement et de recherche français ou étrangers, des laboratoires publics ou privés.

Thermoelectric properties of the homologous compounds $\text{Pb}_5\text{Bi}_6\text{Se}_{14-x}\text{I}_x$

($x = 0.0, 0.025$ and 0.05)

S. Sassi¹, C. Candolfi¹, A. Dauscher¹, B. Lenoir^{1,*}

¹ *Institut Jean Lamour, UMR 7198 CNRS – Université de Lorraine, Parc de Saurupt, CS*

50840, F-54011 NANCY Cedex, France

*Corresponding author: bertrand.lenoir@univ-lorraine.fr

ABSTRACT

Homologous compounds represent an interesting platform for the design of new thermoelectric materials. Here, we report on the synthesis, structural and chemical characterizations and high-temperature transport properties measurements (300 – 700 K) of the $\text{Pb}_5\text{Bi}_6\text{Se}_{14-x}\text{I}_x$ ($x = 0.0, 0.025$ and 0.05) homologous compounds. The successful insertion of iodine into the crystal structure of $\text{Pb}_5\text{Bi}_6\text{Se}_{14}$ was confirmed by its influence on the transport properties. The doping effectiveness of iodine is demonstrated by the increase in the electron concentration resulting in a more pronounced metallic character of transport with respect to undoped $\text{Pb}_5\text{Bi}_6\text{Se}_{14}$. The peak ZT value of 0.5, which was achieved at 700 K in the $x = 0.025$ sample, remains similar to that obtained in $\text{Pb}_5\text{Bi}_6\text{Se}_{14}$.

Keywords: Thermoelectric, homologous compounds, selenides

INTRODUCTION

Since the early 1990s, renewed interest in thermoelectricity has appeared due to the emergence of environmental concerns regarding gases used in refrigeration and greenhouse gas emissions that contribute to global warming [1-3]. Alongside renewable energies, thermoelectricity can play an important role in our everyday life. Indeed, this technology represents one of the alternative solutions to produce electricity from various waste-heat sources. However, the efficiency of the devices, the price and abundance of the elements of the thermoelectric materials are the major drawbacks that confine thermoelectricity to niche technologies such as the power supply of NASA's deep-space probes. The efficiency of a thermoelectric device depends directly on the material transport properties (electrical resistivity, thermal conductivity and thermoelectric power) through the dimensionless factor of merit ZT [1-3]. Optimizing the efficiency of a device thus amounts to increasing the ZT factor at a given absolute temperature T .

In this context, cannizzarite compounds meet several of the requirements to be interesting candidates for thermoelectric applications such as semiconducting properties and very low lattice thermal conductivity [4,5]. In particular, the series $(\text{PbSe})_5(\text{Bi}_2\text{Se}_3)_{3m}$ ($m = 1, 2, 3$ and 4), a subfamily of cannizzarites, has received particular attention in recent years not only for its thermoelectric properties but also for its topologically non-trivial electronic properties for $m = 2$ [6-15]. The $m = 1$ compound crystallizes with a monoclinic structure (space group $P2_1/m$) that contains 50 atoms [6,7,13,14,15]. Its crystal structure, described in detail in prior studies [13,14,15], consists of alternating PbSe layers and m layers of Bi_2Se_3 (Figure 1). This compound exhibits extremely low lattice thermal conductivity values associated with n -type semiconducting properties leading to a maximum ZT value of 0.5 at 723 K [6,7]. These results suggest that further enhancement could be achieved through an

optimization of its electron concentration using appropriate dopants. Prior studies on the binary PbTe have shown that iodine is an effective n -type dopant to control the electron concentration and to optimize the ZT values [16-18].

Here, we show that iodine can be successfully inserted into the crystal structure of the $m = 1$ compound and also behaves as an n -type dopant. The metallic character of the transport is reinforced with the addition of iodine as demonstrated by a concomitant decrease in both the electrical resistivity and thermopower. Despite its doping effectiveness, the solubility limit, estimated to be around 0.025, is too low to further enhance the thermoelectric performances of the $m = 1$ compound. However, our findings demonstrate the chemical flexibility of this homologous compound and suggest that other dopants might be more effective in optimizing its ZT values.

EXPERIMENTAL DETAILS

The phase diagram of the pseudo-binary system PbSe–Bi₂Se₃, which was studied in detail by Zemskov *et al.* [14], indicates that the ternary compound Pb₅Bi₆Se₁₄ can be synthesized by direct solid-state reaction of the precursors PbSe and Bi₂Se₃. For the synthesis of polycrystalline samples of Pb₅Bi₆Se_{14-x}I_x with $x = 0.0, 0.025$ and 0.05 , the two precursors PbSe_{1-x}I_x ($x = 0.0, 0.005$ and 0.01) and Bi₂Se₃ were synthesized. As a first step, pure components (Pb 99.999%, PbI₂ 99.99 %, Se 99.999 % and Bi 99.999 %) were weighed in stoichiometric amounts. The components were then loaded in quartz tubes of 18 mm outer diameter and 3 mm thickness. The sealed quartz tubes with the mixture of components (PbI₂ and Se or Bi and Se) were placed in a vertical furnace and heated to 773 K in 19 h and then to 1373 K in 17 h. The temperature was maintained at 1373 K for 12 h. The furnace was rapidly cooled down to room temperature over 2 h.

The phase purity of these precursors was verified by powder X-ray diffraction prior to use. The two precursors were then hand-ground into fine powders and mixed in predetermined proportions to obtain the desired composition. In order to ensure a good contact between the grains of the precursors and to avoid the formation of secondary phases, the mixtures were cold-pressed into pellets, sealed in quartz tubes and reacted at 873 K for 10 days. The obtained ingots were again hand-ground into fine powders and consolidated by spark plasma sintering (SPS) at 873 K for 10 min under a pressure of 80 MPa. The density of the cylindrical pellets (10 mm in diameter, 8 mm in height) was found to be higher than 98% of the theoretical density for all compounds.

Laboratory powder X-ray diffraction (PXRD) measurements were carried out on a Bruker D8 Advance diffractometer in the $\theta/2\theta$ configuration (CuK α 1, $\lambda = 1.540560 \text{ \AA}$) equipped with a LynxEye positive sensitive detector (PSD). All the acquisitions were carried out at 300 K in 2 θ mode. The operating angle range was adjusted from 20° to 80° with a counting step of 0.032°.

For transport properties measurements, bar- and prism-shaped samples were cut both parallel and perpendicular to the pressing direction with a diamond-wire saw. The thermopower and electrical resistivity were measured simultaneously between 300 and 700 K on bar-shaped samples by using a temperature differential method and four-probe method, respectively, with a ZEM-3 system (ULVAC-RIKO). A laser flash method (LFA 427, Netzsch) was used to measure the thermal diffusivity over between 300 and 723 K on prism-shaped samples. The total thermal conductivity κ was then calculated from the thermal diffusivity a , specific heat C_p and the experimental density d by using the relation $\kappa = aC_p d$.

RESULTS AND DISCUSSION

The PXRD patterns for all compounds, shown in Figure 2, were collected on powdered samples before the SPS sintering process. All the diffraction peaks observed in these patterns correspond to those of the parent compound $\text{Pb}_5\text{Bi}_6\text{Se}_{14}$ suggesting that iodine has been successfully inserted into the crystal structure of the $m = 1$ compound. These results point to the absence of secondary phases within the detection limits of this technique. Note that, due to the lamellar structure of this compound, a significant preferential orientation of the grains is present resulting in strong modifications in the intensity of the ($h00$) reflections.

The evolution of the electrical resistivity ρ of this series of samples (Figure 3a) shows that the measured values are significantly lowered upon inserting iodine. While the ρ values of the $x = 0.025$ and 0.05 samples are lower than those of the undoped compound in the parallel direction up to about 400 K, this tendency is reversed beyond this temperature. The increase in the electrical resistivity with x in the parallel direction suggests a degradation of the electron mobility at high temperatures. The difference between the values measured in the perpendicular direction is more pronounced, the presence of iodine resulting in significantly lower values that reach $45 \mu\Omega\cdot\text{m}$ at 300 K for the two compounds $x = 0.025$ and 0.05 . The fact that the electrical resistivity values for these two compounds are identical in this direction would suggest that the limit of solubility of iodine is less than or equal to $x = 0.025$. However, this trend is different in the parallel direction where a difference between the measured values is clearly visible. This difference suggests that the introduction of iodine into the structure significantly increases the anisotropic character of the electronic properties with respect to the unsubstituted compound.

The temperature dependence of the thermopower of these compounds is shown in Figure 3b. These dependences confirm the trend observed in the electrical resistivity, namely

a reinforcement of the metal character with the addition of iodine. Moreover, the increase in the anisotropy in the electrical resistivity is clearly reflected by these data. Compared to the undoped compound, the anisotropy in the thermopower is more pronounced in the presence of iodine. While the anisotropy suggests the existence of a strong asymmetry between the density of states effective masses of electrons and holes, its variation with the iodine content suggests that the electronic band structure does not evolve in a rigid-like manner.

Figure 3c shows the temperature dependence of the total thermal conductivity. The thermal conductivity decreases with temperature for all samples regardless of the direction probed. The κ values measured in the parallel direction are lower than those in the perpendicular direction in the whole temperature range. The anisotropy is thus reversed with respect to the electrical resistivity values. κ is very low with values varying from 0.35 to 0.50 W m⁻¹ K⁻¹ and from 0.55 to 0.85 W m⁻¹ K⁻¹ for the samples measured in the parallel and perpendicular direction, respectively. While κ increases with increasing x in the perpendicular direction, the reversed trend is observed in the parallel direction, that is, a decrease in κ with increasing the iodine content. These opposite variations faithfully reflect the evolution of the electrical resistivity, which results in an increase (decrease) in the electronic contribution in the perpendicular (parallel) direction.

The electronic contribution that was calculated from the Wiedemann-Franz relation is very small compared to the lattice contribution. The Lorenz number, estimated by a single-parabolic band model, range between 2.02×10^{-8} V² K⁻² at 300 K and 1.66×10^{-8} V² K⁻² at 720 K. Due to the high electrical resistivity values, the total thermal conductivity almost entirely reflects the lattice thermal conductivity κ_L , with the electronic contribution being only 0.05 W.m⁻¹.K⁻¹ at 700 K for these two compounds (14% at most of the total thermal conductivity). The κ_L values are very low for both iodine-substituted compounds and reaches

0.33 W m⁻¹ K⁻¹ and 0.4 W m⁻¹ K⁻¹ at 700 K in the parallel and perpendicular direction, respectively.

The combination of the three transport properties leads to the temperature dependence of the ZT shown in Figure 3d. The variations in temperature are similar for all samples in this series. The anisotropy observed on the different transport properties is not fully compensated leading to anisotropic ZT values. The addition of iodine does not enable enhancing the thermoelectric performances of the compound $m = 1$ with ZT values remaining around 0.5 at 700 K in the doped samples.

CONCLUSION

We reported on the successful synthesis of the homologous compound Pb₅Bi₆Se₁₄ doped with iodine. Our results show that doping the precursor PbSe is an effective approach for doping this homologous compound. PXRD analyses do not show secondary phases. The addition of iodine has a significant influence on the transport properties by providing additional electrons to the electronic structure and increasing the anisotropic character of the transport. Despite very low thermal conductivity values (~ 0.4 W m⁻¹ K⁻¹ at 700 K), the electronic properties did not enable further enhancement of the ZT values with a peak ZT of 0.5 at 700 K, similar to that achieved in the undoped compound in prior studies. The present synthetic approach used to dope the Pb₅Bi₆Se₁₄ compound opens interesting possibilities to further tune its transport properties through the insertion of other elements.

REFERENCES

- [1] H.J. Goldsmid, *Thermoelectric Refrigeration* (London: Temple, 1964).
- [2] D.M. Rowe, *Thermoelectrics and Its Energy Harvesting* (Boca Raton: CRC, 2012).
- [3] D.M. Rowe, *Thermoelectrics Handbook, Macro to Nano* (Boca Raton: CRC, 2006).
- [4] A. Olvera, G. Shi, H. Djieutedjeu, A. Page, C. Uher, E. Kioupakis, and P.F.P. Poudeu, *Inorg. Chem.* 54, 746 (2015).
- [5] J. Casamento, J.S. Lopez, N.A. Moroz, A. Olvera, H. Djieutedjeu, A. Page, C. Uher and P.F.P. Poudeu, *Inorg. Chem.* 56, 261 (2017).
- [6] M. Ohta, D.Y. Chung, M. Kunii and M.G. Kanatzidis, *J. Mater. Chem. A* 2, 20048 (2014).
- [7] S. Sassi, V. Ohorodniichuk, C. Gendarme, P. Masschelein, A. Dauscher, C. Candolfi and B. Lenoir, *J. Electron. Mater.* 46, 2790 (2017).
- [8] K. Nakayama, K. Eto, Y. Tanaka, T. Sato, S. Souma, K. Segawa, T. Takahashi, and Y. Ando, *Phys. Rev. Lett.* 109, 236804 (2012).
- [9] K. Nakayama, H. Kimizuka, Y. Tanaka, T. Sato, S. Souma, T. Takahashi, S. Sasaki, K. Segawa, and Y. Ando, *Phys. Rev. B* 92, 100508 (2015).
- [10] L. Fang, C.C. Stoumpos, Y. Jia, A. Glatz, D.Y. Chung, H. Claus, U. Welp, W.-K. Kwok, and M.G. Kanatzidis, *Phys. Rev. B* 90, 020504 (2014).
- [11] K. Segawa, A.A. Taskin and Y. Ando, *J. Solid State Chem.* 221, 196 (2015).
- [12] S. Sasaki, K. Segawa and Y. Ando, *Phys. Rev. B* 90, 220504 (2014).
- [13] L.E. Shelimova, O.G. Karpinskii and V.S. Zemskov, *Inorg. Mater.* 44, 927 (2008).
- [14] V.S. Zemskov, L.E. Shelimova, P.P. Kostantinov, E.S. Avilov, M.A. Kretova, and I.Y. Nikhezina, *Inorg. Mater. Appl. Res.* 2, 405 (2011).
- [15] Y. Zhang, A.P. Wilkinson, P.L. Lee, S.D. Shastri, D. Shu, D.Y. Chung and M.G. Kanatzidis, *J. Appl. Cryst.* 38, 433 (2005).

- [16] R. W. Fritts in *Thermoelectric Materials and Devices*, ed. I.B. Cadoff and E. Miller, Reinhold Pub. Corp., New York, 1960, pp. 143–162.
- [17] D. Snowden, *Insulator and materials for close-spaced thermoelectric modules*, Hi-z technology, inc. for US department of energy technical report, 2003.
- [18] A.D. LaLonde, Y. Pei, and G.J. Snyder, *Energy Environ. Sci.* 4, 2090 (2011).

FIGURE CAPTIONS

Fig. 1. Crystal structure of the $\text{Pb}_5\text{Bi}_6\text{Se}_{14}$ compound projected along the b -axis. The monoclinic unit cell is represented by the blue dashed line. The Pb-Se and Bi-Se layers are shown in green and blue, respectively. The Pb, Bi and Se atoms are represented by red, blue and orange spheres, respectively.

Fig. 2. PXRD patterns of $\text{Pb}_5\text{Bi}_6\text{Se}_{14-x}\text{I}_x$ with $x = 0.0, 0.025$ and 0.05 . The main Bragg reflections of the $x = 0.0$ have been indexed. The inset shows a magnification of the PXRD patterns between 25 and 50° .

Fig. 3. Temperature dependence of the (a) electrical resistivity ρ , (b) thermopower α , (c) total thermal conductivity κ and (d) dimensionless thermoelectric figure of merit ZT for $\text{Pb}_5\text{Bi}_6\text{Se}_{14-x}\text{I}_x$ with $x = 0.0, 0.025$ and 0.05 . The data measured parallel and perpendicular to the pressing direction are represented by filled and open symbols, respectively. In all panels, the solid curves are guides to the eye.

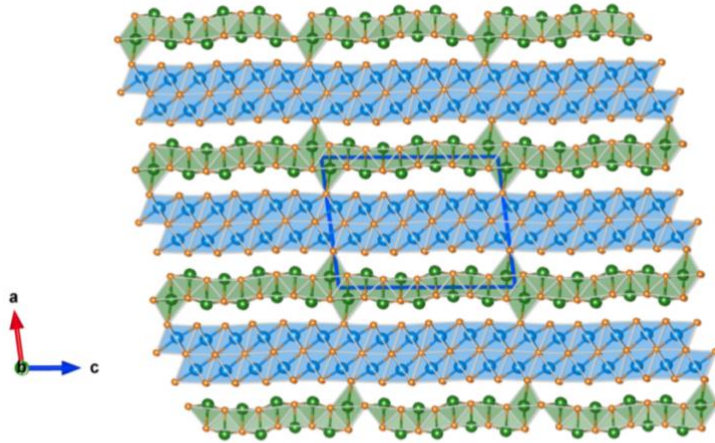


Figure 1

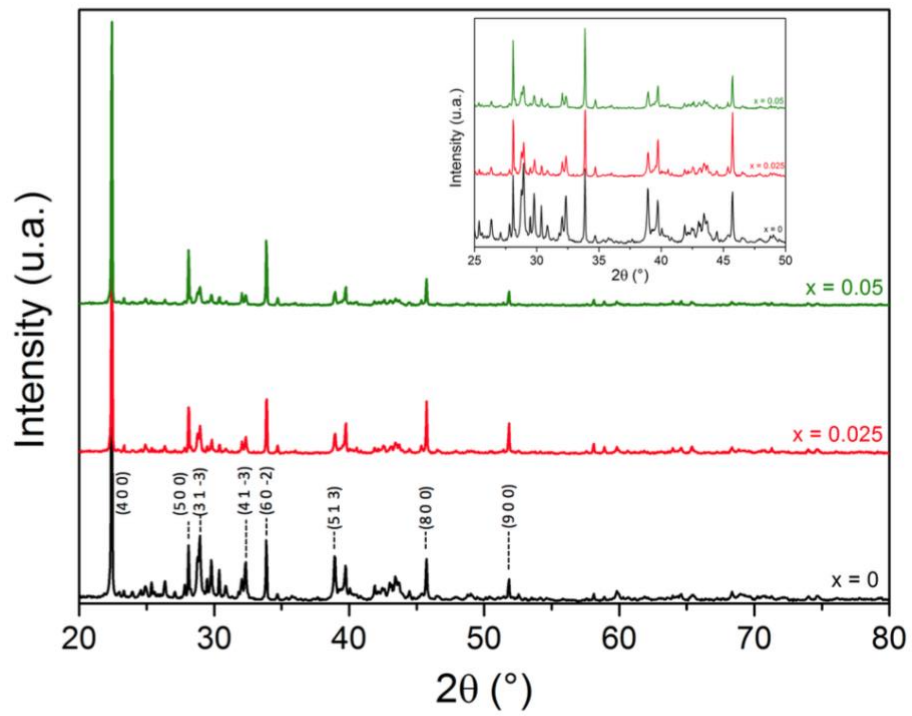


Figure 2

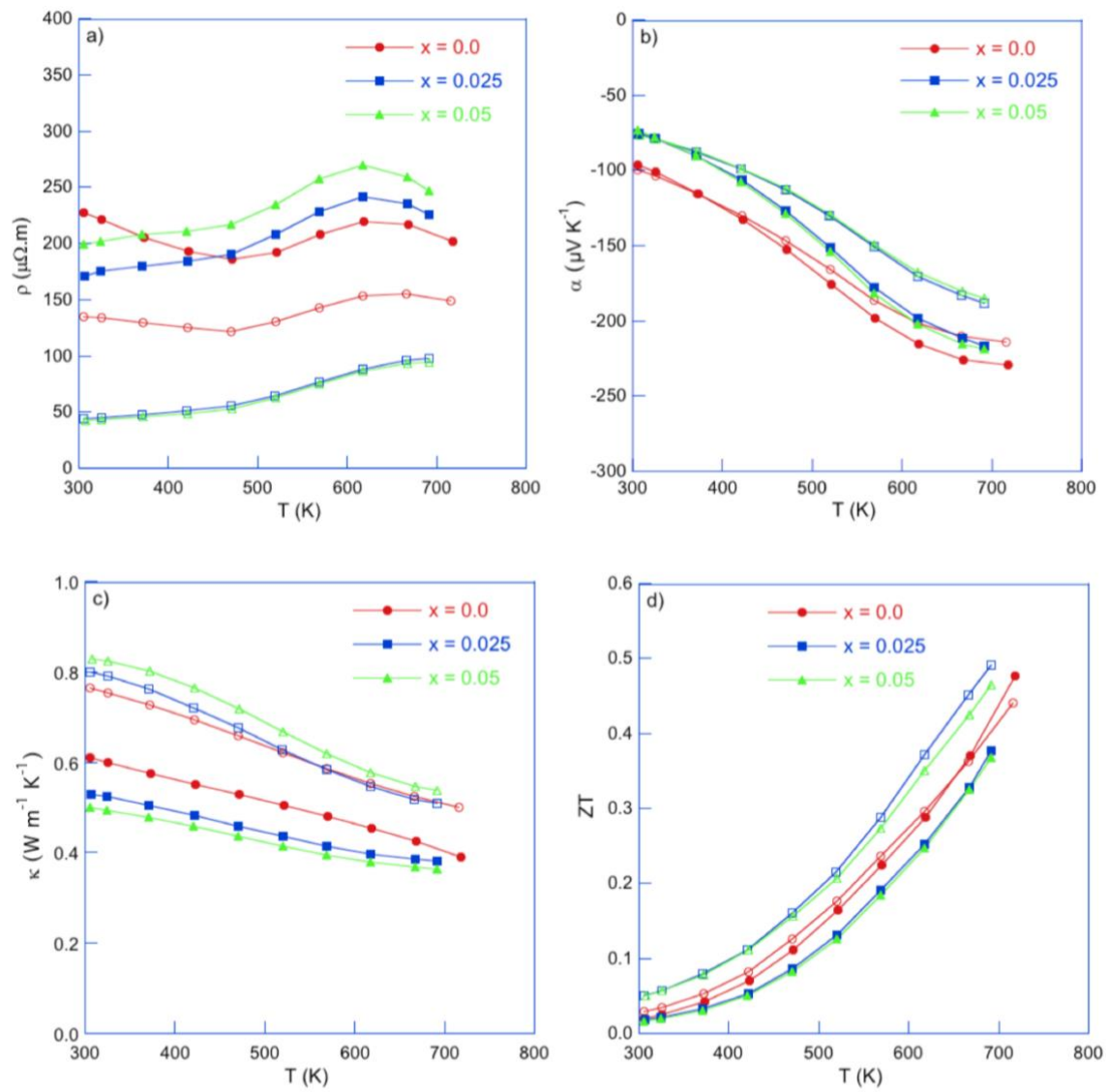


Figure 3